

1 **Spatial and temporal variation in respiratory syncytial virus (RSV) subtype RNA in**
2 **wastewater, and relation to clinical specimens**

3
4 Winnie Zambrana¹, ChunHong Huang², Daniel Solis², Malaya K. Sahoo², Benjamin A. Pinsky^{2,3},
5 Alexandria B. Boehm^{1*}

6
7 1. Department of Civil & Environmental Engineering, Stanford University, 473 Via Ortega,
8 Stanford, CA, USA, 94305

9 2. Department of Pathology, Stanford University School of Medicine, Stanford CA, 94305

10 3. Department of Medicine, Division of Infectious Diseases and Geographic Medicine, Stanford
11 University School of Medicine, Stanford CA, 94305

12

13 *Corresponding author

14 Alexandria B. Boehm, aboehm@stanford.edu, 650-724-9128

15 **Keywords**

16 RSV A, RSV B, wastewater surveillance, subtype variability, subtype monitoring, respiratory syncytial
17 virus

18

19

20 **Abstract**

21 Respiratory syncytial virus (RSV) causes a large burden of respiratory illness, globally. It has two subtypes,
22 RSV A and RSV B, but little is known regarding the predominance of these subtypes during different
23 seasons and their impact on morbidity and mortality. Using molecular methods, we quantified RSV A and
24 RSV B RNA in wastewater solids across multiple seasons and metropolitan areas to gain insight into the
25 predominance of RSV subtypes. We determined the predominant subtype for each group using the
26 proportion of RSV A to total RSV (RSV A + RSV B) in each wastewater sample ($P_{A,WW}$), and conducted a
27 comparative analysis temporally, spatially and against clinical specimens. A median $P_{A,WW}$ of 0.00 in the
28 first season and 0.58 in the second season indicated a temporal shift in the predominant subtype. Spatially,
29 while we observed dominance of the same subtype, $P_{A,WW}$ was higher in some areas ($P_{A,WW} = 0.58$ to 0.88).
30 The same subtype predominated in wastewater and clinical samples, but clinical samples showed higher
31 levels of RSV A (RSV A positivity in clinical samples = 79%, median $P_{A,WW} = 0.58$). These results suggest
32 that wastewater, alongside clinical data, holds promise for enhanced subtype surveillance.

33

34 **Importance.** Respiratory syncytial virus (RSV) causes a large burden of respiratory illness, globally. It has
35 two subtypes, RSV A and RSV B, but little is known regarding the predominance of these subtypes during
36 different seasons and their impact on morbidity and mortality. The study illustrates that information on
37 subtype predominance can be gleaned from wastewater. As a biological composite sample from the entire
38 contributing population, wastewater monitoring of RSV A and B can complement clinical surveillance of
39 RSV.

40

41 1. Introduction

42 Respiratory syncytial virus (RSV) is a leading cause of lower respiratory tract infection across all age
43 groups. Infants, young children, and older adults are the groups with highest risk of developing severe
44 complications from an RSV infection¹. An RSV infection typically causes flu-like symptoms such as
45 congestion, cough and fever, and can cause bronchiolitis and pneumonia in severe cases². Each year in the
46 United States, RSV causes between 58,000 to 80,000 children hospitalizations, and 6,000 to 10,000 older
47 adults deaths^{3,4}. It is estimated that over 100,000 deaths of children under the age of five are attributed to
48 RSV annually globally⁵. The true burden of RSV, however, is substantially underestimated, as such an
49 estimate relies on clinical testing of patients, often only including patients with more severe symptoms
50 that have access to and seek medical treatment. Most older children and adults infected with RSV are
51 excluded from these estimates, as they often only experience mild symptoms⁶. An RSV infection can also
52 be asymptomatic which also contributes to the incomplete understanding of the true burden⁷.

53 RSV is an enveloped, single stranded, negative sense RNA virus that infects humans, and has two
54 subtypes, RSV A and RSV B⁸. The major difference between subtypes is the variation in the G
55 glycoprotein (G protein) that makes up part of the envelope⁹. The pharmaceutical interventions available
56 to combat RSV, such as prophylactic treatments and the recently approved vaccines, consider their
57 difference in structure and can be cross-reactive for both subtypes¹⁰⁻¹². Regardless, these are only
58 available to a limited section of the population (e.g. individuals older than 60 years old, pregnant
59 individuals, and infants younger than 19 months)¹³⁻¹⁷ and have even encountered supply issues^{18,19}.

60 Despite the known structural differences between RSV subtypes, the variability in subtype predominance
61 remains poorly understood. The predominant subtype during an outbreak is often not characterized, as
62 routine surveillance of RSV typically does not include subtype monitoring²⁰. Studies show that although
63 co-circulation of both subtypes is expected, typically one subtype predominates in a particular season²¹.
64 Some epidemiological studies have found that seasons in which RSV A dominated started earlier in the

65 winter, peaked faster, and lasted longer than seasons in which RSV B dominated²², while others found no
66 difference between RSV A- and RSV B-dominated seasons²³. There is also a limited understanding of the
67 difference in virulence between subtypes. Several epidemiological studies found that RSV A was
68 associated with a more severe disease than RSV B, while others reported the opposite or found no
69 difference between them¹⁰. Understanding how subtype predominance varies could aid in discovering
70 potential differences in infection dynamics and virulence caused by each subtype, and could contribute to
71 a better understanding of RSV spread.

72 Wastewater may represent a means for understanding the variability in RSV subtype circulation.
73 Wastewater has recently emerged as a tool for monitoring the disease levels of a community contributing
74 to it, as concentrations of viral genetic material in wastewater have been shown to correlate with
75 positivity rates or clinical case rates for a number of different viruses²⁴⁻²⁷. Several studies have measured
76 RSV RNA wastewater concentrations^{25,28-35}, with only three of them measuring RSV subtypes using
77 PCR-methods^{25,29,30}, and one using a sequence-based methods³². Overall, there is limited research
78 investigating the variability of RSV subtype predominance in wastewater. While some epidemiological
79 studies have studied variations in subtype dominance^{22,23,36,37}, their scope has been confined to clinical
80 samples, typically encompassing individuals with severe RSV cases. This limitation is crucial when
81 considering that the majority of individuals infected with RSV do not seek medical treatment³⁸.
82 Wastewater data bypasses biases inherently included in clinical case data and, thus, could be used to
83 understand variations in RSV subtype predominance at a broader population scale.

84 The goal of this study is to investigate temporal and spatial variations in the predominant RSV subtype
85 detected in wastewater solids samples. This investigation involves measuring concentrations of both RSV
86 A and RSV B in wastewater solids samples across multiple seasons and metropolitan areas, determining
87 the predominant subtype for each, and conducting a comparative analysis temporally, spatially and
88 against clinical data.

89 2. Materials and Methods

90 Study Design

91 This study was carried out at different wastewater treatment facilities across the United States (Table 1),
92 comprising 240 wastewater solids samples in total. The samples in this study are part of a larger
93 wastewater surveillance effort which measures total RSV (RSV A + RSV B) routinely in wastewater
94 solids³⁹, and were selected due to their high total RSV concentration (more information in SI). For each
95 wastewater solids sample, we measured the concentrations of both RSV A and RSV B using digital
96 droplet reverse transcription polymerase chain reaction (RT-PCR), and calculated the main outcome of
97 this study — the proportion of RSV A to total RSV ($P_{A,WW}$):

$$98 \quad P_{A,WW} = C_{RSV A} / (C_{RSV A} + C_{RSV B}) \quad (1)$$

99 where $C_{RSV A}$ is the concentration of RSV A, and $C_{RSV B}$ is the concentration of RSV B in the sample in
100 units of copies/g dry weight. A proportion greater than 0.5, for example, indicates that RSV A is the
101 predominant subtype for that sample. Equation 1 assumes that $C_{RSV Total} = C_{RSV A} + C_{RSV B}$ in each
102 sample. Shedding of RSV A and RSV B by infected individuals into the wastewater stream is assumed to
103 be similar due to the lack of information in the literature⁴⁰.

104 **Table 1.** Characteristics of wastewater treatment plants (WWTPs) included in the study, number of samples per
105 WWTP, sample type, and the evaluations in which they were considered. Settled solids were collected directly from
106 the primary clarifier (“primary clarifier”), or were collected from a raw influent sample (“influent”) and allowed to
107 settle for 10-15 minutes in the laboratory, and later aspirated into a falcon tube using a serological pipette.

WWTP Name	Closest Metropolitan Area	Population Served	Number of samples (Sample dates)	Sample Type	Evaluation
Palo Alto Regional Water Quality Control Plant (PA)	Santa Clara County, CA	236,000	40 (Nov 2021 - Feb 2022) 40 (Nov 2022 - Feb 2023)	Primary clarifier	Temporal, Spatial, Clinical

City of Sunnyvale Water Pollution Control Plant (SV)	Santa Clara County, CA	153,000	40 (Nov 2021 - Feb 2022) 40 (Nov 2022 - Feb 2023)	Primary clarifier	Temporal, Spatial, Clinical
City of Garland Rowlett Creek WWTP (GR)	Dallas, TX	200,000	20 (Nov 2022 - Feb 2023)	Primary clarifier	Spatial
Duck Creek WWTP (DC)	Dallas, TX	186,000	20 (Nov 2022 - Feb 2023)	Primary clarifier	Spatial
RM Clayton Water Reclamation Center (RM)	Atlanta, GA	294,660	20 (Nov 2022 - Feb 2023)	Influent	Spatial
South River Water Reclamation Center (SR)	Atlanta, GA	105,160	20 (Nov 2022 - Feb 2023)	Influent	Spatial

108 *Temporal Evaluation*

109 We compared $P_{A,WW}$ between two different RSV seasons (2021-2022 and 2022-2023) using wastewater
 110 solids samples collected from two WWTPs in the Santa Clara County, CA area (PA and SV) . Samples
 111 from Season 1 (2021-2022) were collected between November 15, 2021 and February 28, 2022, and
 112 samples from Season 2 (2022-2023) were collected between November 1, 2022, and February 28, 2023
 113 (Table 1). The WWTPs included in this evaluation are located 20 kilometers (km) from each other and
 114 have neighboring sewersheds (Figure 1). In a secondary evaluation, we compared results between these
 115 WWTPs within each season to determine if samples from the WWTPs, located in close proximity (~20
 116 km apart with neighboring sewersheds), yield similar results.

117 *Spatial Evaluation*

118 We compared $P_{A,WW}$ between WWTPs located across the United States using wastewater solids samples
 119 collected during a single RSV season (2022-2023). Wastewater solids samples were collected between
 120 November 1, 2022 and February 28, 2023 from three United States areas: Santa Clara County, CA,
 121 Dallas, TX, and Atlanta, GA (Table 1). These areas were selected as they are considered some of the most
 122 populous metropolitan cities in the United States⁴¹, and each have two WWTPs with neighboring

123 sewersheds. Each metropolitan area was represented by two different WWTPs located within 20 km from
124 each other and with neighboring sewersheds. The distances between each metropolitan area were
125 approximately 1,000 km, 2,000 km, and 3,000 km (Figure 1). Note that the samples from Santa Clara
126 County, CA used for this analysis were the same ones used for the temporal variation analysis described
127 above.

128
129



130
131 **Figure 1.** Wastewater treatment plants included in this study. Distance (km) between each of the three metropolitan
132 areas evaluated (A). Distance (km) between both WWTPs selected to represent each area and their corresponding
133 sewersheds: Santa Clara County, California (B), Dallas, Texas (C), and Atlanta, Georgia (D). WWTPs shown in
134 Figure 1B are part of all three evaluations, and WWTPs shown in Figures 1C-1D are only included in the spatial
135 evaluation. This figure was generated using QGIS; map layer from OpenStreetMap (openstreetmap.org/copyright).

136 *Clinical Evaluation*

137 We compared the relative proportion of RSV A identified using wastewater solids ($P_{A,WW}$) to the fraction
138 of clinical specimens collected from individuals residing within and adjacent to the sewersheds in Santa

139 Clara County, CA identified as subtype A ($F_{A,Cl}$). A total of 80 wastewater solids samples and 602
140 clinical samples were included in this evaluation (Table 1), and all were collected in the 2022-2023 RSV
141 season. The wastewater solids samples were already described as those used in the temporal evaluation
142 study. Clinical samples, collected between October 1, and December 31, 2022, were processed by the
143 Stanford Clinical Virology Laboratory (Palo Alto, CA). The laboratory receives samples from patients in
144 the Santa Clara, CA area, including patients living and/or working within the sewershed of the selected
145 WWTPs. This study was conducted with Stanford Institutional Review Board approval (protocol 62834),
146 and individual consent was waived.

147 Using the total number of clinical samples subtyped, we calculated the fraction of clinical specimens
148 identified as subtype A to the total number identified as RSV positive ($F_{A,Cl}$):

$$149 \quad F_{A,Cl} = N_{RSV A} / N_{RSV} \quad (2)$$

150
151
152 where $N_{RSV A}$ is the number of samples that were positive for RSV A, and N_{RSV} is the total number of
153 samples that were subtyped and found positive for either RSV A or RSV B, $N_{RSV} = N_{RSV A} + N_{RSV B}$.
154 $F_{A,Cl}$ was compared to $P_{A,WW}$.

155 *Wastewater solids storage and freeze-thaw cycles impact assessment*

156 Concentrations of pepper mild mottle virus (PMMoV) and total RSV were measured in all wastewater
157 samples immediately after they were collected with no storage (Table S1). To assess the impact of storage
158 and freeze-thaw cycles in our samples, a subset of randomly selected samples ($n = 30$) from Sunnyvale
159 (SV) and Palo Alto (PA) WWTPs were measured a second time for PMMoV after two freeze-thaw
160 cycles. For all samples ($n = 240$), the sum of RSV A and RSV B concentrations taken after two freeze-
161 thaw cycles were compared against the measurements of total RSV in fresh samples.

162 **Statistical Analysis**

163 The median $P_{A,WW}$ of wastewater solids samples were used to compare the predominant subtype between
164 different groups in the statistical analyses. Non-parametric methods were employed as the wastewater
165 data were found to be not normally distributed (Shapiro-Wilk test, $W=0.90$, $p=9.1 \times 10^{-12}$). A Kruskal-
166 Wallis test was used to test the null hypothesis that the $P_{A,WW}$ was not different between groups, and a
167 post-hoc test (Conover-Iman test) was used to compare the $P_{A,WW}$ between groups.

168 A bootstrap method was implemented to compare the $F_{A,Cl}$ to the $P_{A,WW}$. A synthetic dataset consisting of
169 zeros and ones was generated using the total number of clinical samples subtyped (N_{RSV}) and the total
170 number of samples identified as subtype A ($N_{RSV A}$). Next, a collection of 1000 $F_{A,Cl}$ was established by
171 randomly selecting, with replacement, from the synthetic list and calculating it using equation 2. From the
172 collection of 1000 $F_{A,Cl}$, a subset of 80 were randomly selected (equivalent to the number of wastewater
173 solids samples), and subsequently used in the Kruskal-Wallis and post-hoc analyses⁴³.

174 Lastly, three supplementary statistical analyses were performed. Two Kruskal-Wallis tests were
175 conducted to compare fresh sample measurements of RSV and pepper mild mottle virus (PMMoV) with
176 measurements from samples subjected to storage and freeze-thaw cycles to assess the impact of storage
177 on measurements in the wastewater samples. Additionally, Kendall's τ was used to test the null
178 hypothesis that total RSV (RSV A +RSV B) concentration levels and $P_{A,WW}$ are statistically independent.

179 Two hypotheses were tested (two tests: Kruskal-Wallis test and post-hoc test) for each comparison
180 (temporal, spatial or clinical)] and three hypotheses were tested for the supplementary analysis, for a total
181 of 9 hypothesis tests. A p value of 0.006 (0.05/9) for alpha = 0.05 was used to adjust for multiple
182 comparisons (Bonferroni correction). Statistical analysis was completed using R version 4.3.0 within
183 RStudio version 2021.09.1. Wastewater solids data from this study is available at the Stanford Digital
184 Repository⁴⁴.

185 **Procedures**

186 *Wastewater solids sample collection and pre-analytical processing.* Wastewater solids were either grab
187 samples of settled solids from the primary clarifier, or 24-hr composite raw influent samples in which
188 solids were allowed to settle for 10-15 minutes in the laboratory, and aspirated into a falcon tube using a
189 serological pipette (Table 1). Samples were collected in sterile bottles by WWTP staff, immediately
190 stored at 4°C, delivered to the laboratory, and processed within 6 hours upon arrival. Samples were
191 dewatered by centrifugation and resuspended in DNA/RNA shield (Zymo Research, Irvine, CA) spiked
192 with bovine coronavirus vaccine (BCoV, Zoetis, Calf-Guard Cattle Vaccine) to a final concentration of 75
193 mg/ml to minimize inhibition of measurements in solids⁴⁵. Resuspended solids were homogenized and
194 centrifuged, and the supernatant was withdrawn for nucleic-acid extraction. A 0.5 g to 1 g aliquot of the
195 dewatered solids was oven dried to measure its dry weight for its use in the dimensional analysis. Detailed
196 description of the pre-analytical processing can be found elsewhere^{46,47} including in detailed protocols on
197 protocols.io⁴⁷.

198 *Wastewater solids RNA extraction and quantification.* RNA extraction from the supernatant was
199 performed using the Chemagic Viral DNA/RNA 300 kit H96 for the Perkin Elmer Chemagic 360 (Perkin
200 Elmer, Waltham, MA). Extract was further purified using the Zymo One-Step PCR inhibitor removal
201 columns (Zymo Research, Irvine, CA). Nuclease-free water served as a negative extraction control, and
202 BCoV served as a process control. RNA extracts were immediately processed (no storage or freeze-thaw)
203 for quantification of BCoV, pepper mild mottle virus (PMMoV), and total RSV (RSV A + RSV B).
204 Additional aliquots of RNA extracts were stored at -80°C (for 0-700 days) and later subjected to two
205 freeze-thaw cycles for RSV A and RSV B measurements. Although PMMoV was already measured using
206 fresh samples, they were measured again on a subset of the stored and freeze thawed samples to assess the
207 impact of storage and freeze-thaw cycles in our samples (as described in the Study Design section).

208 RNA extracts were used as template neat using one-step RT-ddPCR Advanced Kit for Probes. RSV A
209 and RSV B were measured in a duplex assay using methods described below, and PMMoV, BCoV and
210 total RSV were measured in fresh samples using methods described in detail in other publications³⁹.
211 Primers and probes were purchased from Integrated DNA Technologies (IDT, Coralville, IA). Primers
212 and probe sequences and corresponding thermal cycling conditions were selected from published assays
213 (Table S1)^{25,48-50}. The fluorescence signal was analyzed in the HEX channel for RSV A and the FAM
214 channel for RSV B (Table S1). Nuclease-free water served as a negative PCR control, and gene blocks
215 (Integrated DNA Technologies (IDT), Coralville, IA) served as positive controls for all targets. Non-
216 infectious intact RSV A virus (NATRSVA-STQ, Zeptomatrix, Buffalo, NY) and non-infectious intact
217 RSV B virus (NATRSVB-STQ, Zeptomatrix, Buffalo, NY) were used as additional positive controls for
218 RSV A and RSV B, correspondingly. RNA target concentrations were measured via digital droplet RT-
219 PCR (RT-ddPCR) using an Automated Droplet Generator (Bio-Rad, Hercules, CA), C1000 Touch (Bio-
220 rad) thermocycler, and a QX200 Droplet Reader (Bio-Rad). Droplets were analyzed using QuantaSoft and
221 QuantaSoft Analysis Pro software. Each sample had three replicate wells. Replicate wells were merged,
222 and were required to have at least 10,000 droplets post-merger. A sample was required to have three or
223 more positive droplets across three merged wells to be scored as positive for a target. The lower detection
224 limit for the RSV A and RSV B assays was approximately 2,200 gc/g dry weight, assuming three positive
225 droplets across merged wells. A detailed description of RNA extraction of resuspended solids,
226 quantification using digital RT-ddPCR, and dimensional analysis used to convert concentrations per
227 reaction to copies per gram of dry weight is described in detail in other publications^{46,51} and on
228 protocols.io^{52,53}.

229 *Clinical samples RNA extraction and quantification.* RSV-positive respiratory samples, including
230 nasopharyngeal, mid-turbinate, and anterior nasal swabs in viral transport media, as well as
231 bronchoalveolar lavage fluid, were extracted on the PerkinElmer Chemagic 360 instrument using the
232 Chemagic viral DNA/RNA 300 Kit H96 according to the manufacturer's recommendations. Samples were

233 extracted from 300 μL and eluted in 60 μL . Samples were identified as positive for either RSV A or RSV
234 B using reverse-transcription qPCR (RT-qPCR). The primer and probe sequences were adapted from the
235 assay described by Wang *et al.* 2019⁵⁴, and modified to include RNase P primers and probe to serve as an
236 internal control (Table S2).

237 RT-qPCR was performed using Invitrogen Superscript III Platinum One-Step qRT-PCR kit (Invitrogen,
238 Carlsbad, CA) on the Bio-rad CFX-96 instrument (Bio-rad, Hercules, CA). Each 25 μL reaction
239 contained 12.5 μL of 2X Buffer, 0.5 μL of enzyme mix, 2 μL of primer/probe mix, and 10 μL of eluate.
240 Cycling conditions were as follows: hold at 52°C for 15 min, 94°C for 2 min, then 45 cycles of 94°C for
241 15 sec, 55°C for 40 sec, and 68°C for 20 sec. The fluorescence signal was analyzed in the FAM (A), Cy5
242 (B), and HEX (internal control: RNase P) channels. Thresholds were set at 3000, 1000, and 200 relative
243 fluorescence units (RFU), respectively. Any exponential amplification curve crossing either the FAM or
244 Cy5 RFU thresholds were interpreted as positive for the corresponding target. Samples were considered
245 to have failed extraction or contain inhibitory substances if RNase P did not amplify at a cycle threshold
246 value ≤ 35 cycles. Samples were considered to be untypable if both RSV A and RSV B were not detected.

247 **3. Results and Discussion**

248 **QA/QC.**

249 Results are reported as suggested by the Environmental Microbiology Minimal Information (EMMI)
250 guidelines (Figure S3-S4)⁵⁵. Negative and positive PCR and extraction controls yielded negative and
251 positive results, respectively. Median BCoV recovery in fresh samples was around 100% (median =
252 110%, IQR = 69%), and PMMoV was stable across fresh samples (median = 1.16×10^9 gc/g, IQR = 1.19
253 $\times 10^9$ gc/g).

254 A comparison of total RSV and PMMoV concentrations reported in this study to concentrations measured
255 in samples with no storage and no freeze-thaw cycles showed an effect on target quantification. The
256 median ratios of RSV and PMMoV in stored to fresh samples were 1.29 (IQR = 0.62, $n = 240$) and 0.40

257 (IQR = 0.41, n = 30), respectively. Although the ratios show less than an order of magnitude difference
258 between measurements in fresh and stored samples, we found that fresh sample measurements for both
259 RSV and PMMoV were significantly different from measurements from those measurements in stored
260 samples (Kruskal-Wallis test, RSV comparison $p=1.60 \times 10^{-3}$; PMMoV comparison $p= 1.69 \times 10^{-10}$). This
261 suggests that storage and freeze thaw might have had an impact on target measurements.

262 We found no significant correlation between concentrations of total RSV and $P_{A,WW}$ (Kendall's τ test, $\tau =$
263 0.09, $z = 2.05$, $p=0.04$). This suggests that the levels of total RSV RNA detected in wastewater are not
264 reflective of the predominance of a specific subtype.

265 **Overall Wastewater and Clinical Samples Results.**

266 All wastewater solids samples were positive for RSV A and/or RSV B, with the exception of three
267 samples that were non-detects for either RSV A or RSV B. Median RSV A concentration across all
268 wastewater samples (n = 240) was 1.31×10^4 gc/g dry weight (IQR = 4.07×10^4 gc/g), and median RSV B
269 concentration was 1.90×10^4 gc/g dry weight (IQR = 2.54×10^4 gc/g) (Figure S1). Overall median $P_{A,WW}$
270 across all seasons and all wastewater treatment plants was 0.47 (IQR = 0.74, n = 237) (Figure S2). A total
271 of 593 of 602 RSV-positive clinical samples were identified as either RSV A or RSV B, and 9 samples
272 were considered untypable. We identified the predominant RSV subtype across multiple wastewater
273 treatment plants and conducted a comparative analysis temporally, spatially, and against clinical
274 specimens.

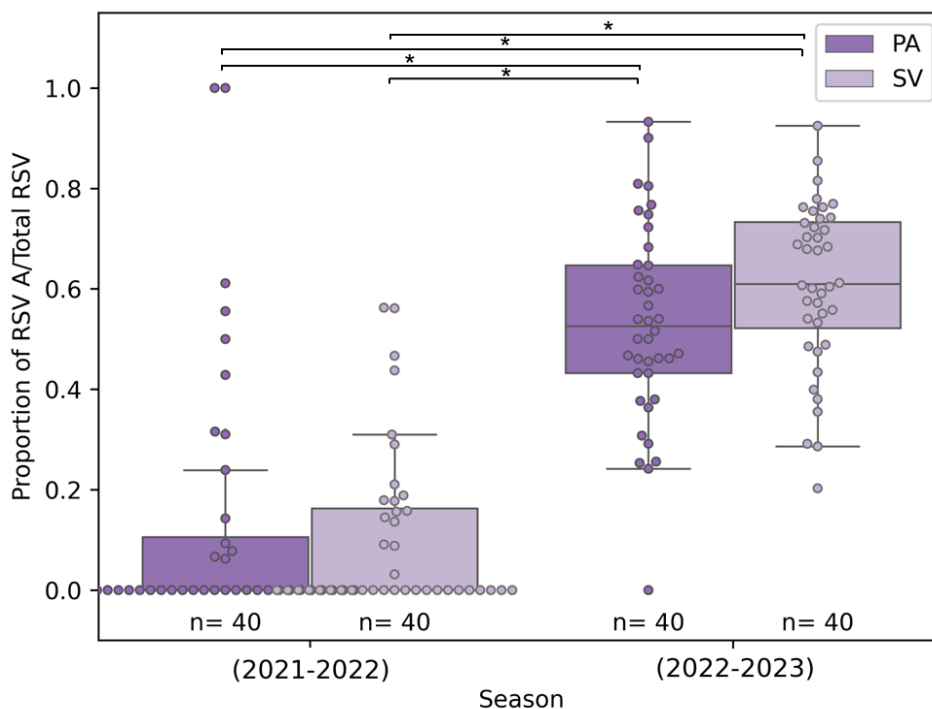
275 **Temporal Evaluation.**

276 The median $P_{A,WW}$ was significantly larger in Season 2 (2022-2023) than Season 1 (2021-2022) for both
277 wastewater treatment plants (Palo Alto Regional Water Quality Control Plant [PA] and City of Sunnyvale
278 Water Pollution Control Plant [SV]) (Conover-Iman test, exact p-values shown in Table S3-S4). The
279 combined median $P_{A,WW}$ from both WWTPs for Season 1 was 0 (PA median = 0.0, IQR = 0.11, n = 40;
280 SV median = 0.0, IQR = 0.16, n = 40), while combined median $P_{A,WW}$ for Season 2 was 0.58 (PA median

281 = 0.53, IQR = 0.21, n = 40; SV median = 0.61, IQR = 0.21, n = 40) (Figure 2, Table S3-S4). The results
282 confirm a change in the predominant subtype between two consecutive RSV seasons. RSV B was the
283 predominant subtype during 2021-2022 with limited RSV A circulation, while in the following season
284 (2022-2023), RSV A dominated with RSV B also circulating.

285 Our results align with epidemiological studies that have also reported shifts in subtype predominance
286 between seasons^{23,36,56}. Observing these results in wastewater solids, which capture contributions from
287 individuals with a wider spectrum of disease severity than clinical data, suggests that changes in subtype
288 dominance between seasons are also observable at the population level. Tracking subtype predominance
289 in wastewater each season could enhance our understanding of RSV dynamics at the population level,
290 particularly when subtype monitoring is not integrated into routine clinical surveillance²⁰.

291 Wastewater treatment plants with neighboring sewersheds (PA and SV) showed similar subtype patterns.
292 For both seasons studied, we found no significant difference in the median $P_{A,WW}$ between each
293 wastewater treatment plant (Conover-Iman test, exact p-values shown in Table S3-S4). This result
294 suggests that if resources are constrained, monitoring one geographic area may provide insights into
295 subtype predominance dynamics in adjacent areas.



296
297 **Figure 2.** Proportion of RSV A to total RSV ($P_{A,WW}$) for the temporal evaluation comparing Palo Alto Regional
298 Water Quality Control Plant (PA) and City of Sunnyvale Water Pollution Control Plant (SV) for Season 1 (2021-
299 2022) and Season 2 (2022-2023). Each box plot is made up of the 25th quartile, median, and 75th quartile
300 proportion of RSV A total RSV for each WWTP per season, and length of each whisker 1.5 times the interquartile
301 range(IQR). Boxplots are overlaid with jittered data points from each group.*= Statistically Significant per post-hoc
302 (Conover–Iman) test with a significance level $p=0.006$ accounting for the Bonferroni Correction.

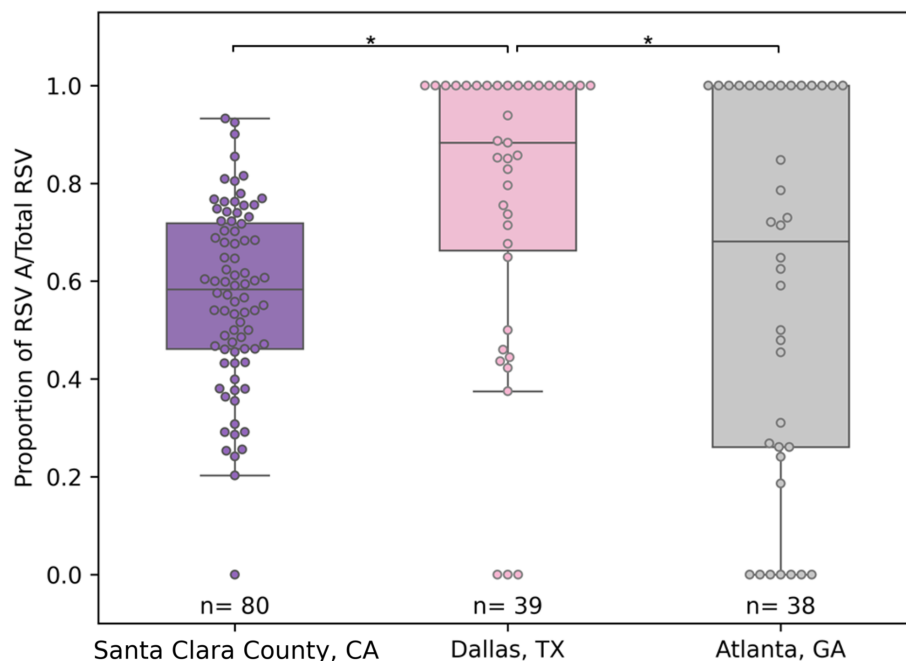
303 Spatial Evaluation.

304 Across the three metropolitan areas evaluated during the 2022-2023 season, RSV subtype A
305 predominated (Santa Clara County, CA median = 0.58, IQR = 0.26, $n = 80$; Dallas, TX median = 0.88,
306 IQR = 0.34, $n = 39$; Atlanta, GA median = 0.68, IQR = 0.74, $n = 38$) (Figure 3). However, the levels at
307 which RSV A was found varied. We found that $P_{A,WW}$ was significantly higher in Dallas, TX than in Santa
308 Clara County, CA and Atlanta, GA, but was similar between Santa Clara County, CA and Atlanta, GA
309 (Conover-Iman test, exact p-values shown in Table S3-S4).

310 Our results, showing dominance of the same RSV subtype across the three metropolitan areas, are
311 consistent with epidemiological studies using clinical samples that have found geographic clustering of

312 viral lineages in large geographical areas (e.g., Australian states)³⁶, and that have concluded that variants
313 are restricted to a local level (i.e., country-wide rather than global)³⁷.

314 Despite sharing a predominant subtype, we observed a lack of association between geographic proximity
315 and levels of one specific subtype. The areas closest to each other (~1,000 km and ~2,000 km apart) were
316 found to have different $P_{A,WW}$, and the two areas with furthest distance from each other (~3,000 km apart)
317 were found to follow similar subtype patterns. Factors beyond physical distance — such as
318 environmental, demographic and transit accessibility factors — may play a crucial role in shaping the
319 levels of subtype dominance. For instance, local climate, minimum temperature, precipitation, and
320 population density have been shown to influence RSV dynamics including onset and timing of peak
321 infectivity^{57,58}, and urban public transportation systems have been shown to facilitate transmission of
322 respiratory illnesses⁵⁹. The three metropolitan areas included in this study experience similar temperate
323 climates with mild winters, but experience different levels of precipitation^{60,61}, have different population
324 densities⁶², and have varying levels of public transportation usage⁶³ which could have contributed to the
325 difference in $P_{A,WW}$.



326
327 **Figure 3.** Proportion of RSV A to total RSV ($P_{A,WW}$) for the spatial evaluation comparing wastewater solids
328 samples from Santa Clara County, CA, Dallas, TX, and Atlanta for Season 2 (2022-2023). Each box plot is made up
329 of the 25th quartile, median, and 75th quartile proportion of RSV A total RSV for two WWTPs per area, and length
330 of each whisker 1.5 times the interquartile range (IQR). Boxplots are overlaid with jittered data points from each
331 group. *= Statistically Significant per post-hoc (Conover–Iman) test with a significance level $p=0.006$ accounting
332 for the Bonferroni Correction.

333 **Clinical Evaluation.**

334 During the 2022-2023 season, 79% (470/593) of the clinical RSV-positive samples were subtyped as
335 RSV A (bootstrapping $F_{A,CI}$ median = 0.79, IQR = 0.03, $n=80$). Wastewater solids samples had a median
336 $P_{A,WW}$ of 0.58 (IQR = 0.26, $n=80$). Therefore, subtype A dominated in both sample types. However, we
337 found the levels of subtype A in clinical samples was significantly higher than in wastewater solids
338 samples (Conover-Iman test, $p=3.88 \times 10^{-26}$) (Table S3-S4).

339 To our knowledge, this is the first study to confirm that wastewater data reflects the same RSV subtype
340 dominance as clinical data. Our results highlight the validity of wastewater as an appropriate
341 epidemiological tool to monitor subtype predominance within a community. The discrepancies in specific
342 subtype levels observed between clinical and wastewater solids samples may stem from the broader
343 representation in wastewater, encompassing mild and asymptomatic cases. Clinical samples, in contrast,

344 might have a larger representation of pediatric infections when considering that children under two are
345 less likely contributors to wastewater solids samples. Wastewater data, in combination with clinical data,
346 could help to provide a comprehensive understanding of the RSV burden.

347 **Limitations and Future Work.**

348 This study has several limitations. First, this study was conducted during atypical RSV periods due to the
349 COVID-19 pandemic and the implementation of nonpharmaceutical interventions. While both seasons
350 began earlier in the year than pre-pandemic levels, the 2021-2022 season lasted longer, and the 2022-2023
351 season exhibited a higher peak number of cases compared to typical RSV epidemics⁶⁴. Another limitation
352 is that we were not able to account for any potential impact of the newly approved vaccines or
353 prophylactic antibody on RSV dynamics, as they were approved for public usage in certain populations
354 subsequent to the 2022-2023 season^{14,16}. Additionally, the temporal evaluation was conducted using data
355 from only two RSV seasons, and the spatial evaluation was limited to three metropolitan areas. A wider
356 range of seasons across a more extensive array of metropolitan areas would enhance our conclusions
357 regarding spatial-temporal subtype predominance. Due to the nature of this retrospective study, another
358 limitation is that wastewater solids samples used to detect RSV subtypes were subjected to storage and
359 freeze thaw which might have had an impact on target measurements. An additional limitation is that the
360 clinical data might also include individuals residing outside the sewershed from the selected WWTPs
361 which could potentially bias the clinical evaluation results. Lastly, although wastewater captures a larger
362 percent of the population infected with RSV than clinical data, it is likely that children under the age of
363 two contribute minimally to wastewater solids samples; therefore, wastewater provides a comprehensive
364 yet incomplete picture of the burden.

365 Despite the aforementioned limitations, the findings in this study suggest that future work regarding RSV
366 subtype variability in several areas is warranted. Future studies could conduct finer-scale temporal
367 evaluations of subtype predominance variability in wastewater, examining potential differences in onset

368 and peak timings between seasons dominated by different subtypes. Spatial evaluations could consider
369 differences in environmental and/or demographic conditions between areas studied that might influence
370 subtype predominance such as climate, precipitation, population density, public transportation usage and
371 other factors. Investigations comparing subtype predominance in wastewater to clinical data could include
372 patient characteristics, distinguishing between pediatric and non-pediatric cases, as well as in-patient vs
373 outpatient cases, to determine the different factors that affect subtype dominance in each signal. Lastly,
374 wastewater monitoring could be integrated into long-term epidemiological studies investigating
375 variability, infection dynamics, virulence characteristics of RSV subtypes, or be used to investigate the
376 effectiveness of the newly approved vaccines at the population level. Wastewater could provide a vital
377 comprehensive picture of cases ranging in severity, and combined with clinical data, could be robust tools
378 to better understand these complex issues.

379 **4. Conclusions**

380 This study presents an analysis of RSV subtypes in wastewater across multiple seasons, metropolitan
381 areas, and in comparison to clinical specimens. We found that the predominant RSV subtype varied
382 temporally, but remained consistent spatially and between wastewater and clinical samples. Temporal
383 evaluation revealed a shift in the predominant subtype between consecutive seasons. Spatially, while we
384 observed dominance of the same subtype across metropolitan areas, the levels of one specific subtype
385 varied, indicating that factors beyond geographic proximity may influence levels of subtype prevalence.
386 When comparing wastewater samples to clinical samples, we found that the same subtype dominated in
387 both sample types, but presence of a specific subtype was higher in clinical samples. Our findings suggest
388 that wastewater, in conjunction with clinical data, holds promise for enhanced subtype surveillance,
389 understanding subtype dynamics, and controlling RSV spread. Future research in RSV subtype
390 predominance can investigate finer-scale temporal variations, study characteristics beyond physical
391 distance, incorporate patient characteristics into clinical-wastewater comparisons, and implement
392 wastewater monitoring into epidemiological studies.

393 5. Supporting Material

394 Additional details about the methods and results used in this study (Tables S1-S4 and Figures S1-S4) .

395 6. Acknowledgements

396 We acknowledge the wastewater treatment plants that kindly provided samples for this study.

397 7. References

- 398 (1) *Respiratory Syncytial Virus (RSV) disease*. World Health Organization.
399 [https://www.who.int/teams/health-product-policy-and-standards/standards-and-](https://www.who.int/teams/health-product-policy-and-standards/standards-and-specifications/vaccine-standardization/respiratory-syncytial-virus-disease)
400 [specifications/vaccine-standardization/respiratory-syncytial-virus-disease](https://www.who.int/teams/health-product-policy-and-standards/standards-and-specifications/vaccine-standardization/respiratory-syncytial-virus-disease) (accessed 2023-
401 07-25).
- 402 (2) *Symptoms and Care for RSV*. Centers for Disease Control and Prevention.
403 <https://www.cdc.gov/rsv/about/symptoms.html> (accessed 2023-07-25).
- 404 (3) *Learn about RSV in Infants and Young Children*. Centers for Disease Control and
405 Prevention. <https://www.cdc.gov/rsv/high-risk/infants-young-children.html> (accessed 2023-
406 07-25).
- 407 (4) *Learn about RSV in older adults with chronic medical conditions*. Centers for Disease
408 Control and Prevention. <https://www.cdc.gov/rsv/high-risk/older-adults.html> (accessed
409 2023-07-25).
- 410 (5) Li, Y.; Wang, X.; Blau, D. M.; Caballero, M. T.; Feikin, D. R.; Gill, C. J.; Madhi, S. A.; Omer,
411 S. B.; Simões, E. A. F.; Campbell, H.; Pariente, A. B.; Bardach, D.; Bassat, Q.; Casalegno,
412 J.-S.; Chakhunashvili, G.; Crawford, N.; Danilenko, D.; Do, L. A. H.; Echavarria, M.;
413 Gentile, A.; Gordon, A.; Heikkinen, T.; Huang, Q. S.; Jullien, S.; Krishnan, A.; Lopez, E. L.;
414 Markić, J.; Mira-Iglesias, A.; Moore, H. C.; Moyes, J.; Mwananyanda, L.; Nokes, D. J.;
415 Noordeen, F.; Obodai, E.; Palani, N.; Romero, C.; Salimi, V.; Satav, A.; Seo, E.;
416 Shchomak, Z.; Singleton, R.; Stolyarov, K.; Stoszek, S. K.; Gottberg, A. von; Wurzel, D.;
417 Yoshida, L.-M.; Yung, C. F.; Zar, H. J.; Abram, M.; Aerssens, J.; Alafaci, A.; Balmaseda,
418 A.; Bandeira, T.; Barr, I.; Batinović, E.; Beutels, P.; Bhiman, J.; Blyth, C. C.; Bont, L.;
419 Bressler, S. S.; Cohen, C.; Cohen, R.; Costa, A.-M.; Crow, R.; Daley, A.; Dang, D.-A.;
420 Demont, C.; Desnoyers, C.; Díez-Domingo, J.; Divarathna, M.; Plessis, M. du; Edgoose,
421 M.; Ferolla, F. M.; Fischer, T. K.; Gebremedhin, A.; Giaquinto, C.; Gillet, Y.; Hernandez, R.;
422 Horvat, C.; Javouhey, E.; Karseladze, I.; Kubale, J.; Kumar, R.; Lina, B.; Lucion, F.;
423 MacGinty, R.; Martinon-Torres, F.; McMinn, A.; Meijer, A.; Milić, P.; Morel, A.; Mulholland,
424 K.; Mungun, T.; Murunga, N.; Newbern, C.; Nicol, M. P.; Odoom, J. K.; Openshaw, P.;
425 Ploin, D.; Polack, F. P.; Pollard, A. J.; Prasad, N.; Puig-Barberà, J.; Reiche, J.; Reyes, N.;
426 Rizkalla, B.; Satao, S.; Shi, T.; Sistla, S.; Snape, M.; Song, Y.; Soto, G.; Tavakoli, F.;
427 Toizumi, M.; Tsedenbal, N.; Berge, M. van den; Vernhes, C.; Mollendorf, C. von; Walaza,
428 S.; Walker, G.; Nair, H. Global, Regional, and National Disease Burden Estimates of Acute
429 Lower Respiratory Infections Due to Respiratory Syncytial Virus in Children Younger than
430 5 Years in 2019: A Systematic Analysis. *The Lancet* **2022**, 399 (10340), 2047–2064.
431 [https://doi.org/10.1016/S0140-6736\(22\)00478-0](https://doi.org/10.1016/S0140-6736(22)00478-0).
- 432 (6) Tin Tin Htar, M.; Yerramalla, M. S.; Mo'isi, J. C.; Swerdlow, D. L. The Burden of

- 433 Respiratory Syncytial Virus in Adults: A Systematic Review and Meta-Analysis. *Epidemiol.*
434 *Infect.* **148**, e48. <https://doi.org/10.1017/S0950268820000400>.
- 435 (7) Munywoki, P. K.; Koech, D. C.; Agoti, C. N.; Bett, A.; Cane, P. A.; Medley, G. F.; Nokes, D.
436 J. Frequent Asymptomatic Respiratory Syncytial Virus Infections During an Epidemic in a
437 Rural Kenyan Household Cohort. *J. Infect. Dis.* **2015**, *212* (11), 1711–1718.
438 <https://doi.org/10.1093/infdis/jiv263>.
- 439 (8) Carvajal, J. J.; Avellaneda, A. M.; Salazar-Ardiles, C.; Maya, J. E.; Kalergis, A. M.; Lay, M.
440 K. Host Components Contributing to Respiratory Syncytial Virus Pathogenesis. *Front.*
441 *Immunol.* **2019**, *10*, 2152. <https://doi.org/10.3389/fimmu.2019.02152>.
- 442 (9) Yu, J.-M.; Fu, Y.-H.; Peng, X.-L.; Zheng, Y.-P.; He, J.-S. Genetic Diversity and Molecular
443 Evolution of Human Respiratory Syncytial Virus A and B. *Sci. Rep.* **2021**, *11* (1), 12941.
444 <https://doi.org/10.1038/s41598-021-92435-1>.
- 445 (10) Vandini, S.; Biagi, C.; Lanari, M. Respiratory Syncytial Virus: The Influence of Serotype
446 and Genotype Variability on Clinical Course of Infection. *Int. J. Mol. Sci.* **2017**, *18* (8),
447 1717. <https://doi.org/10.3390/ijms18081717>.
- 448 (11) Hashimoto, K.; Hosoya, M. Neutralizing Epitopes of RSV and Palivizumab Resistance in
449 Japan. *Fukushima J. Med. Sci.* **2017**, *63* (3), 127–134. <https://doi.org/10.5387/fms.2017-09>.
- 451 (12) Che, Y.; Gribenko, A. V.; Song, X.; Handke, L. D.; Efferen, K. S.; Tompkins, K.; Kodali, S.;
452 Nunez, L.; Prasad, A. K.; Phelan, L. M.; Ammirati, M.; Yu, X.; Lees, J. A.; Chen, W.;
453 Martinez, L.; Roopchand, V.; Han, S.; Qiu, X.; DeVincenzo, J. P.; Jansen, K. U.; Dormitzer,
454 P. R.; Swanson, K. A. Rational Design of a Highly Immunogenic Prefusion-Stabilized F
455 Glycoprotein Antigen for a Respiratory Syncytial Virus Vaccine. *Sci. Transl. Med.* **2023**, *15*
456 (693), eade6422. <https://doi.org/10.1126/scitranslmed.ade6422>.
- 457 (13) *RSV information for healthcare providers*. Centers for Disease Control and Prevention.
458 <https://www.cdc.gov/rsv/clinical/index.html> (accessed 2023-07-10).
- 459 (14) Commissioner, O. of the. *FDA Approves First Respiratory Syncytial Virus (RSV) Vaccine*.
460 FDA. [https://www.fda.gov/news-events/press-announcements/fda-approves-first-
461 respiratory-syncytial-virus-rsv-vaccine](https://www.fda.gov/news-events/press-announcements/fda-approves-first-respiratory-syncytial-virus-rsv-vaccine) (accessed 2023-06-29).
- 462 (15) Regan, A. That Respiratory Infection You Had That Wasn't COVID Has Never Had a
463 Vaccine—until Now. *Fortune Well*. [https://fortune.com/well/2023/05/10/is-there-an-rsv-
464 vaccine-arexvy-gsk-fda-approval/](https://fortune.com/well/2023/05/10/is-there-an-rsv-vaccine-arexvy-gsk-fda-approval/) (accessed 2023-06-29).
- 465 (16) Jewett, C. F.D.A. Approves Pfizer's R.S.V. Vaccine for Older Adults. *The New York Times*.
466 May 31, 2023. [https://www.nytimes.com/2023/05/31/health/fda-rsv-vaccine-older-
467 adults.html](https://www.nytimes.com/2023/05/31/health/fda-rsv-vaccine-older-adults.html) (accessed 2023-07-10).
- 468 (17) *RSV (Respiratory Syncytial Virus) Immunizations* | CDC. Centers for Disease Control and
469 Prevention. <https://www.cdc.gov/vaccines/vpd/rsv/index.html> (accessed 2023-12-26).
- 470 (18) Miller, S. G.; Edwards, E. As RSV Cases Tick up, CDC Warns That a Key Drug to Keep
471 Babies Safe Is in Short Supply. *NBC News*. October 23, 2023.
472 [https://www.nbcnews.com/health/health-news/rsv-cases-tick-key-drug-keep-babies-safe-
473 short-supply-cdc-warns-rcna121763](https://www.nbcnews.com/health/health-news/rsv-cases-tick-key-drug-keep-babies-safe-short-supply-cdc-warns-rcna121763) (accessed 2023-12-26).
- 474 (19) Park, A. What to Know About the RSV Treatment Shortage. *TIME*. November 2, 2023.
475 <https://time.com/6330543/rsv-treatment-shortage/> (accessed 2023-12-26).
- 476 (20) *RSV Surveillance Data - NREVSS* | CDC.
477 <https://www.cdc.gov/surveillance/nrevss/rsv/index.html> (accessed 2024-02-14).
- 478 (21) Borchers, A. T.; Chang, C.; Gershwin, M. E.; Gershwin, L. J. Respiratory Syncytial Virus—
479 A Comprehensive Review. *Clin. Rev. Allergy Immunol.* **2013**, *45* (3), 331–379.
480 <https://doi.org/10.1007/s12016-013-8368-9>.
- 481 (22) Yu, J.; Liu, C.; Xiao, Y.; Xiang, Z.; Zhou, H.; Chen, L.; Shen, K.; Xie, Z.; Ren, L.; Wang, J.
482 Respiratory Syncytial Virus Seasonality, Beijing, China, 2007–2015. *Emerg. Infect. Dis.*
483 **2019**, *25* (6), 1127–1135. <https://doi.org/10.3201/eid2506.180532>.

- 484 (23) Staaedegaard, L.; Meijer, A.; Rodrigues, A. P.; Huang, S.; Cohen, C.; Demont, C.; van
485 Summeren, J.; Caini, S.; Paget, J. Temporal Variations in Respiratory Syncytial Virus
486 Epidemics, by Virus Subtype, 4 Countries. *Emerg. Infect. Dis.* **2021**, *27* (5), 1537–1540.
487 <https://doi.org/10.3201/eid2705.204615>.
- 488 (24) Graham, K. E.; Loeb, S. K.; Wolfe, M. K.; Catoe, D.; Sinnott-Armstrong, N.; Kim, S.;
489 Yamahara, K. M.; Sassoubre, L. M.; Mendoza Grijalva, L. M.; Roldan-Hernandez, L.;
490 Langenfeld, K.; Wigginton, K. R.; Boehm, A. B. SARS-CoV-2 RNA in Wastewater Settled
491 Solids Is Associated with COVID-19 Cases in a Large Urban Sewershed. *Environ. Sci.*
492 *Technol.* **2021**, *55* (1), 488–498. <https://doi.org/10.1021/acs.est.0c06191>.
- 493 (25) Boehm, A. B.; Hughes, B.; Duong, D.; Chan-Herur, V.; Buchman, A.; Wolfe, M. K.; White,
494 B. J. Wastewater Concentrations of Human Influenza, Metapneumovirus, Parainfluenza,
495 Respiratory Syncytial Virus, Rhinovirus, and Seasonal Coronavirus Nucleic-Acids during
496 the COVID-19 Pandemic: A Surveillance Study. *Lancet Microbe* **2023**, *4* (5), e340–e348.
497 [https://doi.org/10.1016/S2666-5247\(22\)00386-X](https://doi.org/10.1016/S2666-5247(22)00386-X).
- 498 (26) Wolfe, M. K.; Duong, D.; Bakker, K. M.; Ammerman, M.; Mortenson, L.; Hughes, B.; Arts,
499 P.; Luring, A. S.; Fitzsimmons, W. J.; Bendall, E.; Hwang, C. E.; Martin, E. T.; White, B.
500 J.; Boehm, A. B.; Wigginton, K. R. Wastewater-Based Detection of Two Influenza
501 Outbreaks. *Environ. Sci. Technol. Lett.* **2022**, *9* (8), 687–692.
502 <https://doi.org/10.1021/acs.estlett.2c00350>.
- 503 (27) Wolfe, M. K.; Yu, A. T.; Duong, D.; Rane, M. S.; Hughes, B.; Chan-Herur, V.; Donnelly, M.;
504 Chai, S.; White, B. J.; Vugia, D. J.; Boehm, A. B. Use of Wastewater for Mpox Outbreak
505 Surveillance in California. *N. Engl. J. Med.* **2023**, *388* (6), 570–572.
506 <https://doi.org/10.1056/NEJMc2213882>.
- 507 (28) Hughes, B.; Duong, D.; White, B. J.; Wigginton, K. R.; Chan, E. M. G.; Wolfe, M. K.;
508 Boehm, A. B. Respiratory Syncytial Virus (RSV) RNA in Wastewater Settled Solids
509 Reflects RSV Clinical Positivity Rates. *Environ. Sci. Technol. Lett.* **2022**, *9* (2), 173–178.
510 <https://doi.org/10.1021/acs.estlett.1c00963>.
- 511 (29) Toribio-Avedillo, D.; Gómez-Gómez, C.; Sala-Comorera, L.; Rodríguez-Rubio, L.;
512 Carcereny, A.; García-Pedemonte, D.; Pintó, R. M.; Guix, S.; Galofré, B.; Bosch, A.;
513 Merino, S.; Muniesa, M. Monitoring Influenza and Respiratory Syncytial Virus in
514 Wastewater. Beyond COVID-19. *Sci. Total Environ.* **2023**, *892*, 164495.
515 <https://doi.org/10.1016/j.scitotenv.2023.164495>.
- 516 (30) Ahmed, W.; Bivins, A.; Stephens, M.; Metcalfe, S.; Smith, W. J. M.; Sirikanchana, K.;
517 Kitajima, M.; Simpson, S. L. Occurrence of Multiple Respiratory Viruses in Wastewater in
518 Queensland, Australia: Potential for Community Disease Surveillance. *Sci. Total Environ.*
519 **2023**, *864*, 161023. <https://doi.org/10.1016/j.scitotenv.2022.161023>.
- 520 (31) Hayes, E. K.; Gouthro, M. T.; LeBlanc, J. J.; Gagnon, G. A. Simultaneous Detection of
521 SARS-CoV-2, Influenza A, Respiratory Syncytial Virus, and Measles in Wastewater by
522 Multiplex RT-qPCR. *Sci. Total Environ.* **2023**, *889*, 164261.
523 <https://doi.org/10.1016/j.scitotenv.2023.164261>.
- 524 (32) Allen, D. M.; Reyne, M. I.; Allingham, P.; Levickas, A.; Bell, S. H.; Lock, J.; Coey, J. D.;
525 Carson, S.; Lee, A. J.; McSparron, C.; Nejad, B. F.; McKenna, J.; Shannon, M.; Li, K.;
526 Curran, T.; Broadbent, L. J.; Downey, D. G.; Power, U. F.; Groves, H. E.; McKinley, J. M.;
527 McGrath, J. W.; Bamford, C. G. G.; Gilpin, D. F. Genomic Analysis and Surveillance of
528 Respiratory Syncytial Virus (RSV) Using Wastewater-Based Epidemiology (WBE).
529 medRxiv July 24, 2023, p 2023.07.21.23293016.
530 <https://doi.org/10.1101/2023.07.21.23293016>.
- 531 (33) Koureas, M.; Mellou, K.; Vontas, A.; Kyritsi, M.; Panagoulas, I.; Koutsolioutsou, A.;
532 Mouchtouri, V. A.; Speletas, M.; Paraskevis, D.; Hadjichristodoulou, C. Wastewater Levels
533 of Respiratory Syncytial Virus Associated with Influenza-like Illness Rates in Children—A
534 Case Study in Larissa, Greece (October 2022–January 2023). *Int. J. Environ. Res. Public.*

- 535 *Health* **2023**, 20 (6), 5219. <https://doi.org/10.3390/ijerph20065219>.
- 536 (34) Rector, A.; Bloemen, M.; Thijssen, M.; Pussig, B.; Beuselinck, K.; Van Ranst, M.; Wollants,
537 E. Respiratory Viruses in Wastewater Compared with Clinical Samples, Leuven, Belgium.
538 *Emerg. Infect. Dis.* **2024**, 30 (1), 141–145. <https://doi.org/10.3201/eid3001.231011>.
- 539 (35) Mercier, E.; Pisharody, L.; Guy, F.; Wan, S.; Hegazy, N.; D'Aoust, P. M.; Kabir, M. P.;
540 Nguyen, T. B.; Eid, W.; Harvey, B.; Rodenburg, E.; Rutherford, C.; Mackenzie, A. E.;
541 Willmore, J.; Hui, C.; Paes, B.; Delatolla, R.; Thampi, N. Wastewater-Based Surveillance
542 Identifies Start to the Pediatric Respiratory Syncytial Virus Season in Two Cities in Ontario,
543 Canada. *Front. Public Health* **2023**, 11, 1261165.
544 <https://doi.org/10.3389/fpubh.2023.1261165>.
- 545 (36) Robertson, M.; Eden, J.-S.; Levy, A.; Carter, I.; Tulloch, R. L.; Cutmore, E. J.; Horsburgh,
546 B. A.; Sikazwe, C. T.; Dwyer, D. E.; Smith, D. W.; Kok, J. The Spatial-Temporal Dynamics
547 of Respiratory Syncytial Virus Infections across the East–West Coasts of Australia during
548 2016–17. *Virus Evol.* **2021**, 7 (2), veab068. <https://doi.org/10.1093/ve/veab068>.
- 549 (37) Agoti, C. N.; Otieno, J. R.; Ngama, M.; Mwihuri, A. G.; Medley, G. F.; Cane, P. A.; Nokes,
550 D. J. Successive Respiratory Syncytial Virus Epidemics in Local Populations Arise from
551 Multiple Variant Introductions, Providing Insights into Virus Persistence. *J. Virol.* **2015**, 89
552 (22), 11630–11642. <https://doi.org/10.1128/jvi.01972-15>.
- 553 (38) Rozenbaum, M. H.; Begier, E.; Kurosky, S. K.; Whelan, J.; Bem, D.; Pouwels, K. B.;
554 Postma, M.; Bont, L. Incidence of Respiratory Syncytial Virus Infection in Older Adults:
555 Limitations of Current Data. *Infect. Dis. Ther.* **2023**, 12 (6), 1487–1504.
556 <https://doi.org/10.1007/s40121-023-00802-4>.
- 557 (39) Zulli, A.; Varkila, M. R. J.; Parsonnet, J.; Wolfe, M. K.; Boehm, A. B. Observations of
558 Respiratory Syncytial Virus (RSV) Nucleic Acids in Wastewater Solids Across the United
559 States in the 2022–2023 Season: Relationships with RSV Infection Positivity and
560 Hospitalization Rates. *ACS EST Water* **2024**. <https://doi.org/10.1021/acsestwater.3c00725>.
- 561 (40) Lowry, S. A.; Wolfe, M. K.; Boehm, A. B. Respiratory Virus Concentrations in Human
562 Excretions That Contribute to Wastewater: A Systematic Review and Meta-Analysis. *J.*
563 *Water Health* **2023**, 21 (6), 831–848. <https://doi.org/10.2166/wh.2023.057>.
- 564 (41) Bureau, U. C. *Large Southern Cities Lead Nation in Population Growth*. Census.gov.
565 [https://www.census.gov/newsroom/press-releases/2023/subcounty-metro-micro-](https://www.census.gov/newsroom/press-releases/2023/subcounty-metro-micro-estimates.html)
566 [estimates.html](https://www.census.gov/newsroom/press-releases/2023/subcounty-metro-micro-estimates.html) (accessed 2024-01-16).
- 567 (42) Esri; TomTom; Garmin; FAO; NOAA; USGS; © OpenStreetMap contributors; GIS User
568 Community. Light Gray Canvas Base, 2017.
569 https://basemaps.arcgis.com/arcgis/rest/services/World_Basemap_v2/VectorTileServer
570 (accessed 2024-03-05).
- 571 (43) Walters, S. J.; Campbell, M. J. The Use of Bootstrap Methods for Analysing Health-
572 Related Quality of Life Outcomes (Particularly the SF-36). *Health Qual. Life Outcomes*
573 **2004**, 2, 70. <https://doi.org/10.1186/1477-7525-2-70>.
- 574 (44) Zambrana, W.; Huang, C.; Solis, D.; Sahoo, M. K.; Pinsky, B. A.; Boehm, A. B. Data on
575 Spatial and Temporal Variation in Respiratory Syncytial Virus (RSV) Subtype RNA in
576 Wastewater, and Relation to Clinical Specimens. **2024**.
577 <https://doi.org/10.25740/jb062yw6825>.
- 578 (45) Huisman, J. S.; Scire, J.; Caduff, L.; Fernandez, -Cassi Xavier; Ganesanandamoorthy, P.;
579 Kull, A.; Scheidegger, A.; Stachler, E.; Boehm, A. B.; Hughes, B.; Knudson, A.; Topol, A.;
580 Wigginton, K. R.; Wolfe, M. K.; Kohn, T.; Ort, C.; Stadler, T.; Julian, T. R. Wastewater-
581 Based Estimation of the Effective Reproductive Number of SARS-CoV-2. *Environ. Health*
582 *Perspect.* **2022**, 130 (5), 057011. <https://doi.org/10.1289/EHP10050>.
- 583 (46) Wolfe, M. K.; Topol, A.; Knudson, A.; Simpson, A.; White, B.; Vugia, D. J.; Yu, A. T.; Li, L.;
584 Balliet, M.; Stoddard, P.; Han, G. S.; Wigginton, K. R.; Boehm, A. B. High-Frequency,
585 High-Throughput Quantification of SARS-CoV-2 RNA in Wastewater Settled Solids at Eight

- 586 Publicly Owned Treatment Works in Northern California Shows Strong Association with
587 COVID-19 Incidence. *mSystems* **2021**, *0* (0), e00829-21.
588 <https://doi.org/10.1128/mSystems.00829-21>.
- 589 (47) Topol, A.; Wolfe, M.; White, B.; Wigginton, K.; Boehm, A. B. *High Throughput pre-*
590 *analytical processing of wastewater settled solids for SARS-CoV-2 RNA analyses.*
591 *protocols.io*. [https://www.protocols.io/view/high-throughput-pre-analytical-processing-of-](https://www.protocols.io/view/high-throughput-pre-analytical-processing-of-waste-b2kmqcu6)
592 [waste-b2kmqcu6](https://www.protocols.io/view/high-throughput-pre-analytical-processing-of-waste-b2kmqcu6) (accessed 2022-04-15).
- 593 (48) Decaro, N.; Elia, G.; Campolo, M.; Desario, C.; Mari, V.; Radogna, A.; Colaianni, M. L.;
594 Cirone, F.; Tempesta, M.; Buonavoglia, C. Detection of Bovine Coronavirus Using a
595 TaqMan-Based Real-Time RT-PCR Assay. *J. Virol. Methods* **2008**, *151* (2), 167–171.
596 <https://doi.org/10.1016/j.jviromet.2008.05.016>.
- 597 (49) Zhang, T.; Breitbart, M.; Lee, W. H.; Run, J.-Q.; Wei, C. L.; Soh, S. W. L.; Hibberd, M. L.;
598 Liu, E. T.; Rohwer, F.; Ruan, Y. RNA Viral Community in Human Feces: Prevalence of
599 Plant Pathogenic Viruses. *PLOS Biol.* **2005**, *4* (1), e3.
600 <https://doi.org/10.1371/journal.pbio.0040003>.
- 601 (50) Haramoto, E.; Kitajima, M.; Kishida, N.; Konno, Y.; Katayama, H.; Asami, M.; Akiba, M.
602 Occurrence of Pepper Mild Mottle Virus in Drinking Water Sources in Japan. *Appl. Environ.*
603 *Microbiol.* **2013**, *79* (23), 7413–7418. <https://doi.org/10.1128/AEM.02354-13>.
- 604 (51) Boehm, A. B.; Wolfe, M. K.; White, B. J.; Hughes, B.; Duong, D.; Banaei, N.; Bidwell, A.
605 Human Norovirus (HuNoV) GII RNA in Wastewater Solids at 145 United States
606 Wastewater Treatment Plants: Comparison to Positivity Rates of Clinical Specimens and
607 Modeled Estimates of HuNoV GII Shedders. *J. Expo. Sci. Environ. Epidemiol.* **2023**.
608 <https://doi.org/10.1038/s41370-023-00592-4>.
- 609 (52) Topol, A.; Wolfe, M.; Wigginton, K.; White, B.; Boehm, A. High Throughput RNA Extraction
610 and PCR Inhibitor Removal of Settled Solids for Wastewater Surveillance of S... **2021**.
- 611 (53) Topol, A.; Wolfe, M.; White, B.; Wigginton, K.; Boehm, A. B. High Throughput SARS-COV-
612 2, PMMOV, and BCoV Quantification in Settled Solids Using Digital RT-PCR. **2022**.
- 613 (54) Wang, L.; Piedra, P. A.; Avadhanula, V.; Durigon, E. L.; Machabishvili, A.; López, M.-R.;
614 Thornburg, N. J.; Peret, T. C. T. Duplex Real-Time RT-PCR Assay for Detection and
615 Subgroup-Specific Identification of Human Respiratory Syncytial Virus. *J. Virol. Methods*
616 **2019**, *271*, 113676. <https://doi.org/10.1016/j.jviromet.2019.113676>.
- 617 (55) Borchardt, M. A.; Boehm, A. B.; Salit, M.; Spencer, S. K.; Wigginton, K. R.; Noble, R. T.
618 The Environmental Microbiology Minimum Information (EMMI) Guidelines: qPCR and
619 dPCR Quality and Reporting for Environmental Microbiology. *Environ. Sci. Technol.* **2021**,
620 *55* (15), 10210–10223. <https://doi.org/10.1021/acs.est.1c01767>.
- 621 (56) Reese, P. E.; Marchette, N. J. Respiratory Syncytial Virus Infection and Prevalence of
622 Subgroups A and B in Hawaii. *J. Clin. Microbiol.* **1991**, *29* (11), 2614–2615.
623 <https://doi.org/10.1128/jcm.29.11.2614-2615.1991>.
- 624 (57) Pitzer, V. E.; Viboud, C.; Alonso, W. J.; Wilcox, T.; Metcalf, C. J.; Steiner, C. A.; Haynes, A.
625 K.; Grenfell, B. T. Environmental Drivers of the Spatiotemporal Dynamics of Respiratory
626 Syncytial Virus in the United States. *PLOS Pathog.* **2015**, *11* (1), e1004591.
627 <https://doi.org/10.1371/journal.ppat.1004591>.
- 628 (58) Zheng, Z.; Pitzer, V. E.; Warren, J. L.; Weinberger, D. M. Community Factors Associated
629 with Local Epidemic Timing of Respiratory Syncytial Virus: A Spatiotemporal Modeling
630 Study. *Sci. Adv.* **2021**, *7* (26), eabd6421. <https://doi.org/10.1126/sciadv.abd6421>.
- 631 (59) Guo, Z.; Xiao, G.; Wang, Y.; Li, S.; Du, J.; Dai, B.; Gong, L.; Xiao, D. Dynamic Model of
632 Respiratory Infectious Disease Transmission in Urban Public Transportation Systems.
633 *Heliyon* **2023**, *9* (3), e14500. <https://doi.org/10.1016/j.heliyon.2023.e14500>.
- 634 (60) *AHPS Precipitation Analysis*. <https://water.weather.gov/precip/> (accessed 2024-01-08).
- 635 (61) *National Maps | National Centers for Environmental Information (NCEI)*. National Oceanic
636 and Atmospheric Administration. <https://www.ncei.noaa.gov/access/monitoring/us-maps/>

- 637 (accessed 2024-01-08).
638 (62) U.S. Census Bureau. *Census Bureau Data*. <https://data.census.gov/> (accessed 2024-01-
639 08).
640 (63) U.S. Department of Transportation. Federal Highway Administration. Status of the Nation's
641 Highways, Bridges, and Transit: Conditions and Performance, 24th Edition.
642 <https://doi.org/10.21949/1521794>.
643 (64) Hamid, S.; Winn, A.; Parikh, R.; Jones, J. M.; McMorrow, M.; Prill, M. M.; Silk, B. J.;
644 Scobie, H. M.; Hall, A. J. Seasonality of Respiratory Syncytial Virus — United States,
645 2017–2023. *MMWR Morb. Mortal. Wkly. Rep.* **2023**, 72 (14), 355–361.
646 <https://doi.org/10.15585/mmwr.mm7214a1>.

647

648

649

650